6th IFAC Symposium Advances in Automotive Control
Munich, Germany, July 12-14, 2010

Design of semi-active steering damper control strategies for sport motorcycles ⋆

P. De Filippi * **M. Tanelli** * **M. Corno** ** **S.M. Savaresi** *
L. Fabbri ***

* *Dipartimento di Elettronica e Informazione, Politecnico di Milano Piazza Leonardo da Vinci, 32 - 20133 Milano, Italy*
** *Center for Systems and Control, Delft University of Technology, Mekelweg 2, 2628 CD Delft, The Netherlands.*
*** *Piaggio Group, Aprilia Brand, Via Galileo Galilei 1, 30033 Noale, Venice, Italy.*

Topic 1 - Vehicle Dynamics

Abstract: This work presents the design of a novel control approach for a semi-active steering damper of motorcycles. The goal is to improve two-wheeled vehicles steering stability by damping the weave and wobble modes. The proposed control strategies stem from a parallelism between steering and vertical dynamics of a motorcycle. According to this parallelism, the Sky-Hook and Ground-Hook damping concepts are adapted to the control of steering dynamics. A detailed analysis of the two approaches is presented and the semi-active control strategies are shown to yield better attenuation of both modes than a passive steering damper. Further, both a multi-body simulator and experimental data are employed to validate the proposed control approach.

Keywords: Motorcycle dynamics, Semi-active dampers, Control systems design, Steering dynamics.

1. INTRODUCTION AND MOTIVATION

It is well known that two-wheeled vehicles can become difficult to control because of the low damping of some of their characteristic modes. Experimental observation and mathematical modeling show that there are two principal modes of vibration under straight-running and steady state cornering conditions: weave and wobble (see Cossalter [2002], Limebeer et al. [2002]). Weave is a low frequency oscillation of the entire motorcycle. Wobble is a higher frequency oscillation of the steering handle around its axis. These modes can become lightly damped or even unstable under certain operating conditions. When they approach the instability boundary, weave and wobble are difficultly controllable by the rider as the former affects the entire motorcycle and the latter has a natural frequency higher than the physiological bandwidth of the rider.

In the scientific literature the analysis of the steering dynamics has been addressed by several works, see for example Evangelou et al. [2007], Sharp and Limebeer [2004], Cossalter et al. [2002], Tanelli et al. [2009]. In these works multi-body models serve as a basis of modal and sensitivity analyses showing that wobble and weave depend on many parameters, both static (such as caster angle, wheel base and wheel inertia) and dynamic (roll angle and forward velocity). It is also shown that adding a passive steering damper (a device that produces a moment opposite to the angular velocity of the steering assembly relative to the vehicle frame) can improve weave and wobble damping. The tuning of such a device is not straightforward, as shown by Figures 1(a)-1(b), which plot the frequency response $G_{T_s\delta}(j\omega)$ from steering torque to steering angle at different forward velocities. The frequency responses are identified from data obtained with simulations performed using Bikesim^{TM}, a full-fledged commercial motorcycle simulation environment based on the AutoSim symbolic multi-body software, tuned to fit a high-performance motorcycle. A constant speed straight run is simulated and a frequency sweep (1-20 Hz) torque disturbance is applied to the steer. This analysis confirm the results by Evangelou et al. [2006] showing that: (i) at low speed only the wobble mode is undamped; at high speed both modes resonances are clearly visible; (ii) a high steering damper coefficient improves the damping of the wobble mode, but is detrimental for that of the weave mode and vice versa.

The above analysis shows that the optimal tuning of a passive steering damper is nontrivial. In the recent past a solution to this problem has been proposed by Evangelou et al. [2007], where a passive mechanical compensator is used to damp the weave and wobble modes. This passive mechanical compensator is composed of a spring, a damper and an inerter. The inerter exerts a force proportional to the relative acceleration of its terminal ends. The authors show that the mechanical compensator ensures improved performance over the entire operating regime. Evangelou and co-authors tested the passive mechanical network in simulation, obtaining promising results. However, the passive mechanical network is technologically complex and has been manufactured exclusively as a prototype.

Well aware of the difficulties involved in finding an optimal tuning of a passive steer damper, motorcycles manufacturers usually employ a tunable passive steering damper that the rider can adjust to his/her likings. In the last few years semi-active switching steering dampers have been introduced, i.e., shock absorbers whose damping coefficient can be changed from a minimum (c_{min}) to a maximum (c_{max}) value. In this context, a static map is implemented to adapt the damping coefficient, which is increased with forward speed and acceleration. According to the previous analysis this yields an attenuation of the wobble mode

⋆ The work of P. De Filippi, M. Tanelli and S.M. Savaresi has been partially supported by the MIUR project "New methods for Identification and Adaptive Control for Industrial Systems" and by the Piaggio Group S.p.A..

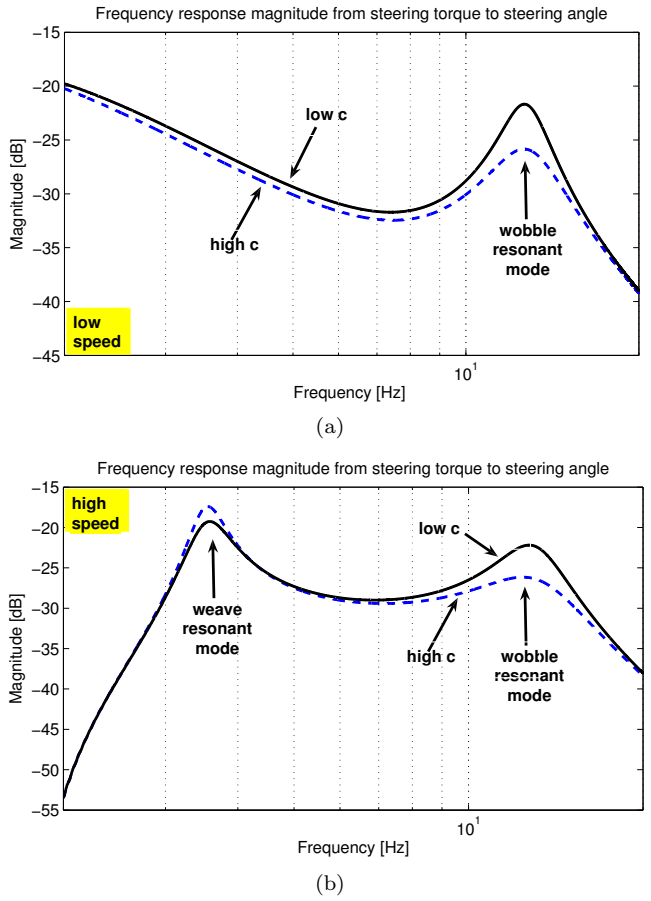

Fig. 1. Plot of the magnitude of the frequency response $G_{T_s\delta}(j\omega)$ with roll angle $\varphi = 0^o$ and (a) speed $v = 50$ km/h and (b) speed $v = 140$ km/h; maximum (dashed line) and minimum (solid line) steer damper value.

but an amplification of the weave resonance. Thus, these adaptive control strategies do not take full advantage of the capability of a semi-active steering damper.

The scope of this paper is the analysis and the design of industrially amenable switching semi-active control strategies for steering dampers aimed at improving the damping of weave and wobble modes. The analysis of the weave and wobble analytical model reveals a parallelism between vertical and steering dynamics; this analogy is exploited to adapt the concept of Sky-Hook and Ground-Hook, developed in the control of vertical dynamics (see e.g., Fischer and Isermann [2004], Savaresi et al. [2003], Williams [1997]), to motorcycle steering dynamics. Two control laws are therefore designed: the Rotational-Ground-Hook, aimed at minimizing the absolute vibration of the steering axis, and the Rotational-Sky-Hook aimed at damping the chassis oscillations. It is then shown that the two solutions can improve weave and wobble damping. Finally, experimental tests on an instrumented bike are carried out to assess the validity of the proposed controllers.

The paper is structured as follows: Section 2 recalls the analytical model of the steering dynamics. Section 3 discusses the design of the semi-active control strategies and the simulation results while in Section 4 the experimental results are presented.

2. STEERING DYNAMICS ANALYSIS

In this section the description of the motorbike steering dynamics is derived starting from the control-oriented model presented in Tanelli et al. [2009]. The vehicle is comprised of two bodies: the main frame and the steering assembly. These can rotate around the steering axis. Figures 2(a)-2(b) provide a side-view and a view from above of the vehicle with the needed notation. In what follows, c_θ and s_θ stand for $\cos(\theta)$ and $\sin(\theta)$, respectively.

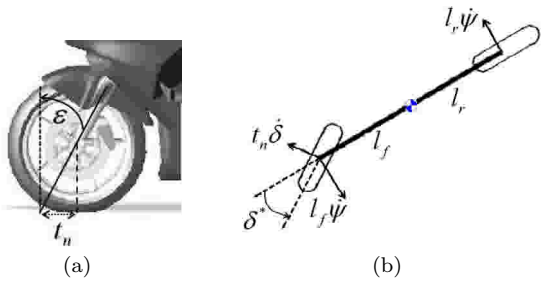

(a) (b)

Fig. 2. Side view (left) and view form above (right) of the motorbike with reference frames and notation

The model is derived based on the following assumptions.

- The forward speed v is constant.
- The tire longitudinal force exerted by the tire is equal to zero: tire rolling friction and aerodynamics drag are neglected.
- The tire moments are neglected as their contribution is very small.
- The variations of tire side-slip angles and roll angles around the nominal condition are small.
- The product of inertia between the steering assembly and the main frame is neglected.
- The gyroscopic effects are neglected.
- The motorcycle is assumed in straight run with null lateral acceleration.

Under the above assumptions, the torque balances of the out-of-plane modes can be derived. The torque balance computed around the vertical axis is written as

$$J_z\ddot{\psi} - F_{yf}l_f c_{\delta^*} + F_{yr}l_r = 0, \tag{1}$$

where J_z is the yaw inertia, $\ddot{\psi}$ is the yaw acceleration, F_{yf} and F_{yr} are the tire lateral forces, l_f and l_r are the distances between the center of mass and the front and rear tire, respectively, and $\delta^* = \delta c_\epsilon$ (see Figure 2(b)) is the angle between the vehicle and the tire longitudinal axis due to a steering manoeuver possibly while cornering.

The torque balance around the steering axis yields

$$J_s\ddot{\delta} + c\dot{\delta} + F_{yf}t_n = T_s, \tag{2}$$

where J_s is the steer inertia, T_s is the steering torque, t_n is the normal trail and c is the steering damping coefficient. Assuming small variations of the tire side-slip angles around the nominal condition, the tire lateral forces can be written as

$$F_{yi} = N_i\, k_{\alpha_i}\alpha_i, \quad i = \{f, r\}, \tag{3}$$

where N_i is the vertical load acting on the tire, k_{α_i} is the *cornering stiffness* (see e.g., Cossalter [2002]). From Figure 2(b) the side-slip angles at the wheels can be computed as

$$\begin{aligned}\alpha_f &= \psi - \frac{l_f}{v}\dot{\psi} + \frac{t_n}{v}\dot{\delta} + c_\epsilon\delta \\ \alpha_r &= \psi + \frac{l_r}{v}\dot{\psi}.\end{aligned} \tag{4}$$

The described dynamical model can be written in the form

$$\begin{aligned}&M_\phi\ddot{\phi} + R_\phi(\rho)\dot{\phi} + K_\phi\phi = Q_{T_s}T_s, \\ &\phi = [\,\psi\ \ \delta\,]^T,\end{aligned} \tag{5}$$

where

$$M_\phi = \begin{bmatrix} J_z & 0 \\ 0 & J_s \end{bmatrix} \quad (6)$$
$$R_\phi = \frac{1}{v}\begin{bmatrix} N_r K_{\alpha_r} l_r^2 + N_f K_{\alpha_f} l_f^2 & -N_f K_{\alpha_f} l_f t_n \\ -N_f K_{\alpha_f} l_f t_n & cv + N_f K_{\alpha_f} t_n^2 \end{bmatrix}$$
$$K_\phi = \begin{bmatrix} N_r K_{\alpha_r} l_r - N_f K_{\alpha_f} l_f & -N_f K_{\alpha_f} l_f c_\epsilon \\ N_f K_{\alpha_f} t_n & N_f K_{\alpha_f} t_n c_\epsilon \end{bmatrix}$$

are mass, damping and stiffness matrices, and $Q_{T_s} = [0\ 1]^T$. This model has some interesting features.

- The mass matrix is diagonal and positive definite.
- The chassis inertia is larger than the steer one: this is consistent with the fact that the weave mode, associated with the chassis inertia, presents a lower natural frequency than that of the wobble mode, which depends on the steer inertia.
- For all speed values $v > 0$ the damping matrix R_ϕ is symmetric, positive definite and inversely proportional to the forward velocity v.
- The stiffness matrix is not symmetric, because the force field is not conservative. Further, note that the yaw stiffness ($k_{\phi_{11}}$) depends on the difference between front and rear tire stiffness, while the steer stiffness ($k_{\phi_{22}}$) depends only on front tire stiffness and normal trail.

Further considerations can be drawn from the modal matrix analysis. Computing the modal matrix Φ_v for the speed values $v = 50$ and $v = 140$ km/h, and normalizing each column with respect to the element of largest magnitude, one gets

$$\Phi_{50} = \begin{bmatrix} 0.82 & -1 \\ -1 & 0.2 \end{bmatrix},\ \Phi_{140} = \begin{bmatrix} 0.8 & -1 \\ -1 & 0.2 \end{bmatrix}. \quad (7)$$

The modal matrices confirm that the natural frequencies associated with the weave mode are 3.9 Hz at 50 km/h and 3.5 Hz at 140 km/h, while the ones associated with the wobble mode are 8.4 Hz at 50 km/h and 9.5 Hz at 140 km/h. Moreover, the weave mode column presents values of yaw and steer components similar and opposite, while the wobble mode column presents a dominant value of the steer component. These properties are consistent with the observation that when weave is excited the motorcycle exhibits a behavior of the steering assembly and the body which is opposite in phase, whereas the wobble mainly affects the steering axle.

Interestingly, model (5) can be used to draw a parallelism between vertical and steering dynamics of two-wheeled vehicles. The dynamic model of a quarter-car system can be described by the following equations

$$\begin{aligned} &M\ddot{x} + R\dot{x} + Kx = Q_d z_r \\ &x = [\, z\ z_t \,]^T \\ &Q_d = [\, 0\ k_t \,]^T, \end{aligned} \quad (8)$$

where z, z_t and z_r are the vertical position of the body, the unsprung mass and the road profile, respectively. Thus, the mass, damping and stiffness matrix are

$$M = \begin{bmatrix} M & 0 \\ 0 & m \end{bmatrix},\ R = \begin{bmatrix} c & -c \\ -c & c \end{bmatrix},\ K = \begin{bmatrix} k & -k \\ -k & k + k_t \end{bmatrix}, \quad (9)$$

where M is the quarter-car body mass; m is the unsprung mass; c is the damping coefficient; k and k_t are the stiffness of the suspension spring and of the tire, respectively. These matrices have the same structure of those in (6): in particular, the mass matrix is diagonal and its elements are of significantly different magnitude. The body mass M is associated with the resonance of the vehicle chassis, while the unsprung mass m is associated with the wheel resonance. Thus, the body resonance can be linked to the weave resonance, while the wheel resonance is associated with the wobble resonance. Table 1 fully describes the parallelism between the two domains. In the next section, it will be shown how, thanks to this analogy, the concepts of Sky-Hook (SH) and Ground-Hook (GH) can be extended to the out-of-plane steering modes.

Table 1. Variables and Parameters Mapping.

Vertical Dynamics		Steering Dynamics
M	$\longleftrightarrow$	J_z
m	$\longleftrightarrow$	J_s
$\dot{z}$	$\longleftrightarrow$	$\dot{\psi}$
$\dot{z}_t$	$\longleftrightarrow$	$\dot{\delta} + \dot{\psi}$
Δz	$\longleftrightarrow$	δ

3. CONTROL STRATEGIES FOR SEMI-ACTIVE STEERING DAMPERS

The simplified model derived in the previous section shows the similarities between the problem of controlling vertical dynamics and that of controlling steering dynamics. In the vertical dynamics domain, the most commonly used control frameworks are the Sky-Hook (SH) and Ground-Hook (GH) damping (see e.g., Fischer and Isermann [2004], Savaresi et al. [2003], Williams [1997]).

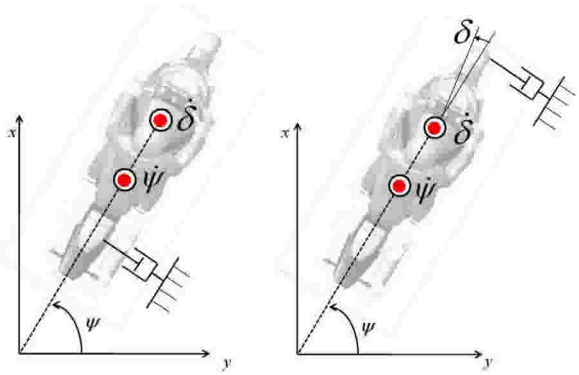

Fig. 3. Schematic view of the ideal Sky-Hook (left) and Ground-Hook (right) damping scheme.

The classical SH is based on an ideal shock absorber connected between the sprung mass and a fixed reference frame in the sky; this idea is extended to the Rotational Sky-Hook (R-SH) strategy (see Figure 3) by ideally fixing a shock-absorber linked to the chassis and to an appropriate frame. This frame translates with the motorcycle and rotates only around longitudinal and transversal axes. The rationale of this configuration is that of isolating the chassis from road or steering torque disturbances. According to this configuration, the ideal shock-absorber should deliver a torque proportional to the chassis yaw rate, that is

$$\tau_{sh}(t) = c_{sh}\dot{\psi}(t), \quad (10)$$

while the actual steering damper delivers a torque proportional to the steering angular velocity, i.e.,

$$\tau(t) = c(t)\dot{\delta}(t). \quad (11)$$

In case of a continuously modulated damping coefficient, the R-SH strategy could be implemented by actuating, at each time instant t, a damping coefficient $c_{in}(t)$ computed by equaling the ideal and the actual torques in (10) and (11). When dealing with two-state dampers, as it is the case considered in this work, $c_{in}(t)$ can take only two values (c_{min} and c_{max}) and the so called two-state

approximation of the R-SH control algorithm must be adopted. This approximation is given by

$$c_{in}(t) = \begin{cases} c_{max} \text{ if } \dot{\psi}(t)\dot{\delta}(t) \geq 0 \\ c_{min} \text{ if } \dot{\psi}(t)\dot{\delta}(t) < 0 \end{cases} . \quad (12)$$

The classical GH is based on an ideal shock absorber connecting the unsprung mass with a fixed reference on the ground; this idea is translated into the Rotational Ground-Hook (R-GH) control strategy (see Figure 3). The R-GH is based on the idea of linking a shock-absorber to the steering assembly and to the same reference frame described for the R-SH case. This configuration guarantees a better damping of the front-assembly in the face of both road and steering torque disturbances. In the R-GH approach, the ideal shock-absorber delivers a torque proportional to the sum of the yaw rate and steering angular velocity, that is

$$\tau_{gh}(t) = c_{gh}\left(\dot{\delta}(t) + \dot{\psi}(t)\right), \quad (13)$$

while the steering damper always delivers the torque computed in (11). By applying the same reasoning as before, the two-state approximation of the R-GH is

$$c_{in}(t) = \begin{cases} c_{max} \text{ if } \dot{\delta}(t)\left(\dot{\delta}(t) + \dot{\psi}(t)\right) \geq 0 \\ c_{min} \text{ if } \dot{\delta}(t)\left(\dot{\delta}(t) + \dot{\psi}(t)\right) < 0 \end{cases} . \quad (14)$$

Finally, note that these control strategies require the measurement of the yaw rate and steering angular velocity. The former can be easily measured via a single axis gyroscope, whereas the latter can be obtained via numerical differentiation of the steering angle measurement.

3.1 Closed-loop Performance Analysis

The performance of the R-SH and R-GH algorithms have been extensively analyzed via simulation tests performed on the BikeSim motorcycle simulator.

Figure 4 plots the frequency responses $G_{T_s\delta}(j\omega)$ at a forward velocity of 140 km/h. Two linear passive steering dampers ($c_{min} = 0.016$ Nm/s and $c_{max} = 0.044$ Nm/s) and the R-SH and R-GH control algorithms have been simulated, using as input a frequency sweep steering torque disturbance, ranging from 1 to 20 Hz.

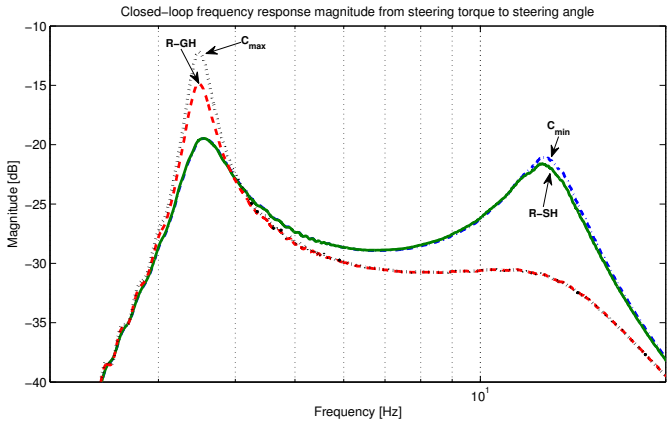

Fig. 4. Magnitude of the closed-loop frequency response $G_{T_s\delta}(j\omega)$ with $\varphi = 0°$ and $v = 140$ km/h: c_{min} (dashed-dotted line), c_{max} (dotted line), R-SH (solid line) and R-GH (dashed line).

By inspecting Figure 4 the following remarks can be made.

- The R-SH algorithm provides an optimal attenuation (as good as the one achieved by c_{min}) around the weave resonance frequency (located at approximately 3.3 Hz) and an intermediate attenuation around the wobble mode (located at approximately 12.5 Hz), slightly better than c_{min}, but not as good as c_{max}.
- The R-GH algorithm provides an optimal damping (as good as that achieved by c_{max}) around the wobble resonance and an intermediate attenuation at low frequency: better than c_{max}, but not as good as c_{min}.

It is also interesting to notice that the two approaches are not symmetric. The difference beetwen the performance of the R-SH and that of c_{min} at high frequency is smaller than the one between R-GH and c_{max} at low frequency. This phenomenon is better understood by analyzing the ideal R-SH and R-GH strategies in (12) and (14) and by recalling that Figure 4 shows the closed-loop performance in the face of a steering torque disturbance. The R-SH, by ideally exerting a torque that is proportional to the chassis yaw rate, tends not to intervene when a high frequency torque is applied on the steering head, as it mainly excites the steering assembly. Conversely, the R-GH strategy ideally exerts a torque proportional to $\left(\dot{\delta} + \dot{\psi}\right)$ and, by doing so, it acts significantly also when the excitation is at low frequency. The situation is different if the disturbance comes from the road surface as shown by Figure 5. In this case the motorcycle performs a steady state turn on a road with a frequency height profile, ranging from 1 to 20 Hz. The plot depicts the frequency response $G_{d\delta}(j\omega)$ from road disturbance d to steering angle δ with roll angle $\varphi = 30°$ and speed $v = 140$ km/h for the different control strategies. Also in this case, it is clear how the proposed control strategies outperform passive approaches. In particular, when the disturbance comes from the road, the difference between R-SH and c_{min} in damping the wobble mode is more evident than it was in the case of the steering torque disturbance. In case of a road disturbance, in fact, a high frequency excitation affects both the vehicle chassis (and hence the yaw rate) and the steering assembly.

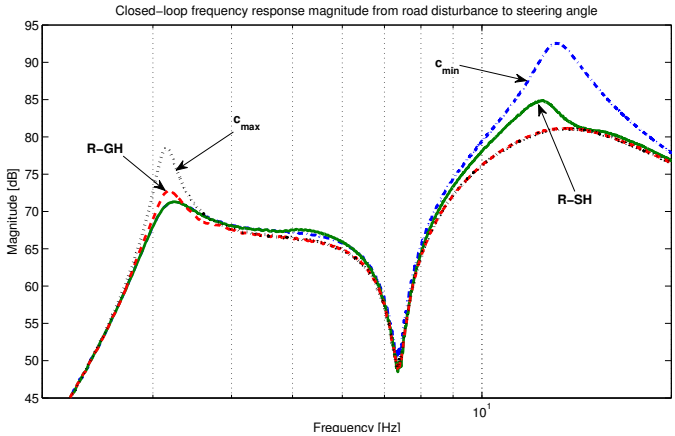

Fig. 5. Magnitude of the closed-loop frequency response $G_{d\delta}(j\omega)$ with $\varphi = 30°$ and $v = 140$ km/h; c_{min}, c_{max}, R-SH (dash-dotted line), R-GH (dashed line).

The frequency responses in Figures 4 and 5 clearly show that, although the semi-active solutions deliver better performance than the passive ones, they are not able of solving the trade-off between weave and wobble damping. In fact, the R-SH approach is natively aimed at damping the weave mode, while the R-GH approach is focused on the wobble mode. This confirms the parallelism between vertical dynamics and steering dynamics. Interestingly, the

parallelism can be pushed even further by noting that in Figure 4 there is a point, called *invariant point*, located at the point of intersection between the frequency responses of the passive solutions c_{min} and c_{max}, which delimits the frequency regions where R-GH outperforms R-SH and *vice versa*. This consideration is currently being investigated to design a control scheme that optimally manages the trade-off.

To provide a concise way to compare the performance of the proposed control algorithms, the road disturbance sweep experiment has been repeated for several velocities between 50 and 200 km/h. For each velocity and control strategy, the following cost function has been computed

$$J_s = \frac{1}{N}\sum_{k=1}^{N}\left(\delta(k) - \overline{\delta}\right)^2 \tag{15}$$

where $\delta(k)$ is the steering angle sample, $\overline{\delta}$ is the steady state steering angle and N is the number of samples in the test. For each speed, J_s is then normalized with respect to the worst case cost function obtained for all the considered passive and semi-active steering controllers. Figure 3.1 shows the average value of the cost functions computed at different forward speeds. By inspecting Figure 3.1 the

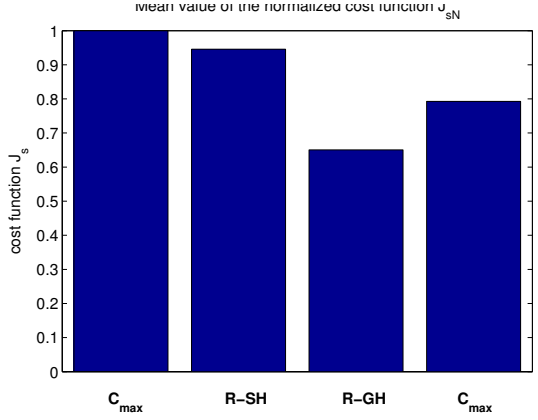

Fig. 6. Mean value of the normalized cost function J_s obtained at different speed.

following remarks can be made.

- Among the two purely passive tunings, c_{max} performs better than c_{min}. This reflects the fact that wobble is present at all speeds, while weave at high speed only.
- R-SH outperforms c_{min}. Even though they both yield roughly the same damping of the weave mode, R-SH offers better performance than c_{min} with respect to the wobble. Namely, an improvement of 6% is noted.
- R-GH outperforms c_{max} as they reach the same damping of the wobble mode, but R-GH can better damp the weave than c_{max}. Namely an improvement of 14% is noted.
- Among all strategies the R-GH algorithm yields the best results. This is a consequence of the vehicle trimming: the considered vehicle is more subject to wobble than to weave, as reflected by the fact that the *invariant point* is at low frequency (circa 4 Hz). Thus R-GH has more margin for improvement with respect to the passive solution than R-SH which tends to damp the weave.

In the present section it has been shown that semi-active steering damper control strategies can improve the stability of the motorcycle with respect to purely passive solutions. Nevertheless, the analysis of the performance in the frequency domain reveals that a trade-off between the weave and wobble damping persists; control strategies that optimize the damping of both weave and wobble are under study.

4. EXPERIMENTAL RESULTS

To experimentally investigate the steering dynamics of sport motorcycles, an hypersport bike propelled by a 1000cc 4-stroke engine has been instrumented. The bike weights about 150 kg (without rider) and can deliver 140 HP. The vehicle has been equipped with

- a linear potentiometer to measure steering angle;
- two wheel encoders to measure the wheels angular velocity;
- a one axis MEMS gyroscope to measure yaw rate;
- a semi-active on/off damper, actuated via a solenoid valve with a bandwidth of approximately 10 Hz.

All the signals are sampled at 1 kHz. To study the dynamic behavior of the steering angle response to steering torque variations, the following test drive was devised: the rider was asked to bring the motorcycle to a given constant forward speed in straight running. After the steady state condition is reached, the rider tries to mimic a double torque impulse signal by violently hitting the handlebars. After this perturbation he was asked to let the bike oscillate with the minimum possible human intervention on the handlebars. The same type of test was repeated at different speeds, ranging from 50 to 140 km/h.

These tests were used to investigate the sensitivity to the damping coefficient of the steering damper. Three configurations have been tested: the minimum and maximum damping of the semi-active damper (c_{min}, c_{max}) and no damping at all (c_0).

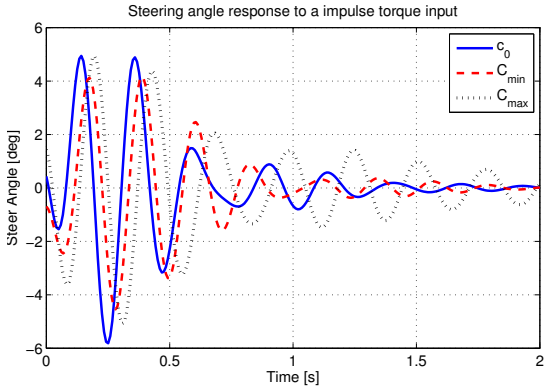

Fig. 7. Time history of the steering angle response to a double-impulse torque input at $v = 140$ km/h: c_0 (solid line), c_{min} (dashed line) and c_{max} (dotted line).

The results in Figure 7 agree with the expected weave mode damping as a function of the damping coefficient (see also Figure1(b)). The oscillations settle more quickly as c decreases. A more objective quantification of the damping was achieved employing Kung's subspace identification algorithm (see e.g. Lovera and Previdi [2000]). Specifically, a linear time-invariant dynamical model has been estimated from the measured impulse responses. Cross-validation tests led to choose a 4^{th} order model, which is consistent with the analytical modeling.

Based on the identified model, the top plot of Figure 8 shows the map of weave model eigenvalues as a function of damping coefficient of the steering damper at a forward speed of 140 km/h. As can be seen, the sensitivity to this parameter is well captured by the model: a steering

damper with nearly null damping coefficient guarantees the best damping.

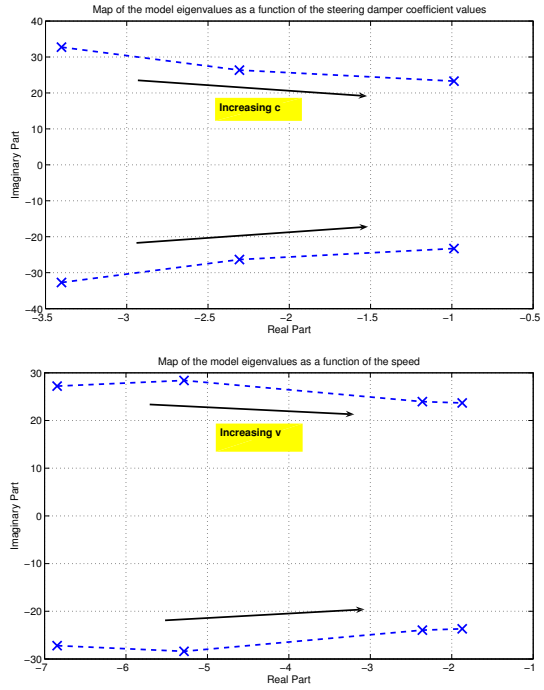

Fig. 8. Map of the model eigenvalues as a function of the steering damper coefficient values c_0, c_{min} and c_{max} at speed $v = 110$ km/h (left) and of the vehicle speed values 50, 80, 110 and 140 km/h for minimum steer damper value c_{min}.

The bottom plot of Figure 8 shows the map of the identified weave eigenvalues as a function of the forward speed, which confirms that the actual weave mode is well damped at low speeds, while it is only slightly damped at high speeds. Thus, the experimentally obtained weave mode characteristics are in good agreement with what discussed in Section 2.

Finally, R-SH and R-GH control strategies were implemented and Figure 9 shows the values of the normalized cost function J_s obtained on experimental data for $v = 110$ km/h. The experimental tests successfully validate the proposed control algorithms. The two semi-active strategies outperform the corresponding purely passive one. It is interesting to note that in the experimental tests R-SH outperforms all other strategies. This can be explained by noting that the experimental tests excite the weave resonance more than the wobble one. Currently, an experimental protocol that safely excites the wobble mode is being devised.

5. CONCLUDING REMARKS AND OUTLOOK

In this paper, the steering dynamics of a two-wheeled vehicle has been studied and discussed, and a parallelism between vertical and steering dynamics control has been proposed. Based on this, innovative control strategies for semi-active steering damper control have been proposed. Specifically, Rotational Sky-Hook and Rotational Ground-Hook algorithms have been worked out which allow to effectively damp the weave and the wobble resonance, respectively. The performance of the control strategies has been evaluated both via a full-fledged motorcycle simulator and with an instrumented vehicle equipped with an on/off semi-active damper. Current research is being

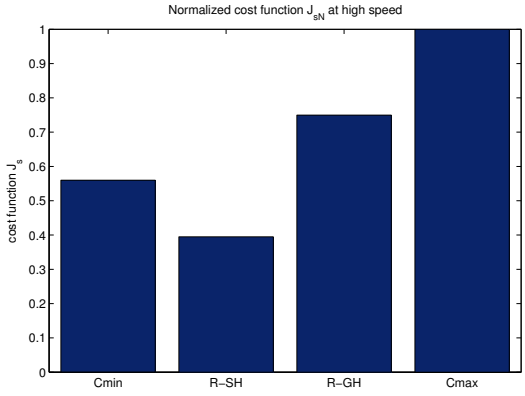

Fig. 9. Values of the normalized cost function J_{sN} for $v = 110$ km/h obtained on experimental data.

focused on the design of control strategies able to optimally damp both weave and wobble modes.

REFERENCES

V. Cossalter. *Motorcycle Dynamics*. Race Dynamics, Milwaukee, USA, 2002.

V. Cossalter, R. Lot, and F. Maggio. The Influence of Tire Properties on the Stability of a Motorcycle in Straight Running and in Curve. In *SAE Automotive Dynamics & Stability Conference (ADSC)*, Detroit, Michigan, USA, May 7-9, 2002.

S. Evangelou, D.J.N. Limebeer, R.S. Sharp, and M.C. Smith. Control of motorcycle steering instabilities. *Control Systems Magazine, IEEE*, 26(5):78–88, Oct. 2006. ISSN 0272-1708. doi: 10.1109/MCS.2006.1700046.

S. Evangelou, David J. N. Limebeer, Robin S. Sharp, and Malcolm C. Smith. Mechanical steering compensators for high-performance motorcycles. *Journal of Applied Mechanics*, 74(2):332–346, 2007.

D. Fischer and R. Isermann. Mechatronic semi-active and active vehicle suspensions. *Control Engineering Practice*, 12(11):1353 – 1367, 2004.

D. J. N. Limebeer, R. S. Sharp, and S. Evangelou. Motorcycle steering oscillations due to road profiling. *Journal of Applied Mechanics*, 69(6):724–739, 2002.

M. Lovera and F. Previdi. Identification of linear models for the dynamics of a photodetector. *Control Engineering Practice*, 8(10):1149 – 1158, 2000.

S.M. Savaresi, E. Silani, S. Bittanti, and N. Porciani. On performance evaluation methods and control strategies for semi-active suspension systems. In *Decision and Control, 2003. Proceedings. 42nd IEEE Conference on*, volume 3, pages 2264–2269 Vol.3, Dec. 2003.

R.S. Sharp and D.J.N. Limebeer. On steering wobble oscillations of motorcycles. *Proceedings of the Institution of Mechanical Engineers, Part C: Journal of Mechanical Engineering Science*, 218(12):1449–1456, 2004.

M. Tanelli, M. Corno, P. De Filippi, S. Rossi, S.M. Savaresi, and L. Fabbri. Control-oriented steering dynamics analysis in sport motorcycles: modeling, identification and experiments. In *15th IFAC Symposium on System Identification (SYSID)*, 2009.

R.A. Williams. Automotive active suspensions part 1: basic principles. In *Proceedings of the Institution of Mechanical Engineers, Part D: Journal of Automobile Engineering*, volume 211, pages 415–426, Dec. 1997.